

# Performance Analysis of a Seamless Sliding Mode Control for a Non Isolated Multi-Input Multi-Output Bidirectional Dc-Dc Boost Converter for Electric Vehicle Applications

<sup>1</sup>J. Ramprabu, <sup>2</sup>K. Deepa

<sup>1</sup>Assistant Professor, Department of Electrical and Electronics Engineering,  
Kumaraguru College of Technology, India

<sup>2</sup>PG Scholar, Department of Electrical and Electronics Engineering,  
Kumaraguru College of Technology, India

<sup>1</sup>ramprabu.j.eee@kct.ac.in, <sup>2</sup>deepakittuswamy@gmail.com

**Abstract:** *In this paper, a non isolated multi-input multi-output dc–dc boost converter is proposed. This converter is used to implant alternative energy sources in electric vehicles. However, advantages of different sources of energy are achievable by the implant energy sources. This converter has many outputs with different voltage levels, which can be interfaced with multilevel inverters. In this converter, the load power can be distributed flexibly between input sources, so that a proper control for charging and discharging of energy storages by other input sources can be achieved in a better manner. Using a multilevel inverter can lead to reduction of voltage harmonics, which in turn, reduces the torque ripple of electric motors in electric vehicles. A Small-signal model for each operation mode is extracted to design the converter control system. A unique sliding mode control with output filter in a smooth manner is used to regulate the bidirectional converter. By using this control strategy stability analysis can be made for both the step-up and step-down operating modes of the converter. In this paper the two types of bidirectional dc–dc converters— cascade buck boost capacitor in the middle and cascade buck boost inductor in the middle are compared and their performance is analyzed based on the parameters such as requirements of devices, switches and components rating, control strategy, and performance analysis for use in plug-in electric and hybrid electric vehicles. The simulation and experimental results are provided for both converter types and the validity of the proposed converter and its stability and the control performance are verified for different operating conditions.*

**Keyword:** *Cascaded buck–boost; DC–DC converters; electric vehicle; hybrid power system; multi-input multi-output (MIMO); small signal modeling;*

## 1. INTRODUCTION

Rapid increase in population and energy consumption in the world, increasing oil and natural gas prices, and the depletion of the fossil fuels is the reasons for the fast emerging of electrical vehicles (EVs) instead of fossil-fuel or non renewable energy source vehicles. The interest in developing the EVs with clean and renewable energy sources as an alternate source of fossil-fuel vehicles is increasing very fast. To provide the environment friendly operation, the EVs are considered as an efficient and attractive solution for transportation applications by the usage of clean and renewable energy sources [1], [2]. In the EVs, the fuel cell is used as clean energy source that directly converts the chemical energy reaction to the electrical energy. At present, FC's is considered as one of the promising technologies that meet the future energy requirements. However, there are some well-known technical drawbacks for which

FCs are not used separately in the EVs to fulfill the demands of the load, particularly during start up and transient events as they have slow power transfer rate in transitory situations, and a high cost per watt. In order to solve these problems, usually the FC is used with energy storage battery systems (ESBSs) such as batteries or super capacitor (SC). Usage of a dc–dc converter for each of the input sources will result in increase in price, mass, and losses. Consequently, in hybrid systems, multi-input dc–dc converters have been used and they are mainly two types, they are isolated multi-input dc–dc converter and non isolated multi-input dc–dc converter.

In [3], a non isolated multi-input dc–dc converter which is derived from H-bridge structure has been discussed. Modes in either output voltage of the H-bridges are negative are not considered. By eliminating the non useful modes, a simplified and

simple double input dc–dc converter is obtained. The less number of passive elements is the main advantage of this converter, and its limitation is unsuitable control of the power which is drawn from input sources. In [4]–[6], a multi-input dc–dc buck converter is discussed, this converter consists of two parallel buck converters in their inputs. Reduced number of inductors and capacitors results in reduction of cost, volume, and weight of converter are the advantage of this converter. Lack of proper power flow control between input sources is the limitation of the proposed converter. In [7], multi-input z-source dc–dc converter's, structure is proposed such that the number of inductors and capacitors is equal to a single input z-source converter. In [8], multiphase converter is proposed and has four inputs by different voltages.

The goal of sliding-mode control is to implement a smooth strategy is a very simple solution to the converter working in a bidirectional mode. Two operation modes are exhibited by the bidirectional DC-DC converters, the step-up mode in which the energy flows from the battery to the motor, and the step-down mode in which the energy flows from the motor to the battery and, therefore helps in regenerative braking. By inserting an additional switching pattern when changing from one mode operation to the other, the smooth variation is achieved. In [9], a sliding-mode control strategy is used in battery storage applications to control the output current of a bidirectional dc-dc buck converter with an output LCL-filter.

The output LCL filter results in a higher attenuation of the high frequency harmonics in the battery current when compared to the usual L-filter. The battery current in both step-up and step-down modes can be controlled by a single-sliding mode controller.

The analyzed and compared dc–dc converter is used for dc fast charging in EV/HEVs to extend the all-electric drive range. In the literature [10]–[12], different types of bidirectional dc–dc converters along with their comparison are proposed and have been analyzed for PHEV charging applications in [12].

Three level bidirectional dc–dc converters have been found to be more efficient when compared with other converters as the output voltage is smoother with three possible values of the output voltage, smaller energy storage devices and low switch voltage stress. The cascaded buck–boost inductor in the middle (CBB-IM) and the cascaded buck–boost capacitor in the middle (CBB-CM) converter is proposed in [13], [14]; the converter topology is shown in Figure 1 and Figure 2.

This paper presents the analysis of these two converters, with experimental evaluation of the converters along with multiple input and multiple output considerations.

## 2. NON ISOLATED CONVERTER STRUCTURE AND ITS OPERATION MODES

The single input converter is proposed in this paper. At the same time, load requirements cannot be met by the use of only one input energy source in electric vehicles. In order to overcome this limitation one inductor is required for implant different energy. In this paper, combination of non isolated multi-input, multi-output dc–dc converters is proposed. It is seen from the figure that the converter has  $n$  input power sources  $V_{i1}, V_{i2}, V_{i3}, \dots, V_{in}$  such as  $V_{i1} < V_{i2} < V_{i3} \dots < V_{in}$ . As specified already, the proposed converter has only one inductor,  $m$  capacitors in its outputs and  $m + n$  switches. The  $R_1, R_2, R_3 \dots R_m$  is the load resistances, in multi level inverter which can represent the equivalent power feeding in it. Power flow control between the input sources in addition to boost up input source voltages is achieved by switching the switches in a proper way. Outputs are capable of having equal or different voltage level which is suitable for connecting to a multilevel inverter. The converter proposed in this paper is suitable for implant the energy storage battery system (ESBSs) such as FC, battery, or Super Capacitor (SC). The converter with two-input two-output is analyzed in this paper for convenience.

The Figure 1 shows the analyzed converter with two-input two-output. Despite of their type many multilevel inverters can be used in connection with this converter but it must be used along with non floating dc-links. Power switches SW1, SW2, SW3, and SW4 in the structure of the converter are the four main control elements that control the output voltages and power flow of the converter. In the given converter, the power can be delivered from source  $V_{i1}$  to source  $V_{i2}$  but not vice versa. So, in EV applications, Fuel Cell which cannot be charged is located where  $V_{i1}$  is placed in circuit. Also, usually where  $V_{i2}$  is placed, ESBSs such as battery or SC which are chargeable are located. In this paper, FC is used as a generating power input source and the battery is used as an ESBS. Depending on the use of the battery, two operating modes are defined and in each mode, only three of the four switches are active, while the other switch is inactive.

When the output power of the load is high, both the source of input deliver power to load, in such a condition, SW2 is inactive and switches SW1, SW3, and SW4 are active. Also, when load power is low and  $V_{i2}$  is needed to be charged,  $V_{i1}$  not only supplies loads but also can charge  $V_{i2}$ . In this condition, switches SW1, SW2, and SW4 are active and SW3 is inactive. In this paper, CCM is used to investigate the steady state and dynamic behavior of the converter. However, the converter works in discontinuous conduction mode (DCM) when the

loads power and battery charging current have low values in battery charging mode.

four different operation modes in one switching period as follows:

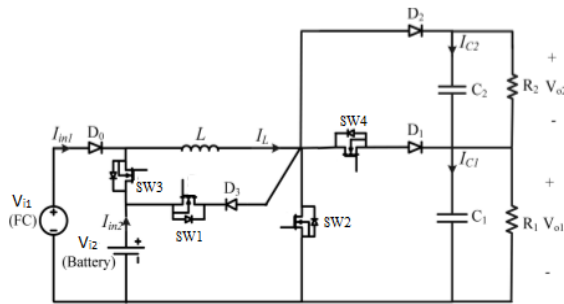


Figure 1 Two input two output non isolated DC-DC converters

Two main operation modes of the converter have been investigated as follows:

## 2.1 First Operation Mode -Battery Discharging Mode (BDCM)

In this mode of operation, two input power sources  $V_{i1}$  and  $V_{i2}$  (battery) are responsible for supplying the loads. In this mode, SW2 is OFF entirely and SW1, SW3, and SW4 are active. A specific duty is considered for each switch. Here, SW1 is active to regulate source 2 (battery) current to desired value. In fact, SW1 controls the inductor current to regulate the battery current to desired value. The duty of the switch SW3 is to regulation the total output voltage  $V_T = V_{O1} + V_{O2}$  to desired value. Similarly, the output voltage  $V_{O1}$  is controlled by SW4. Gate signals, voltage and current waveforms of switches and inductor are shown in Figure 2.

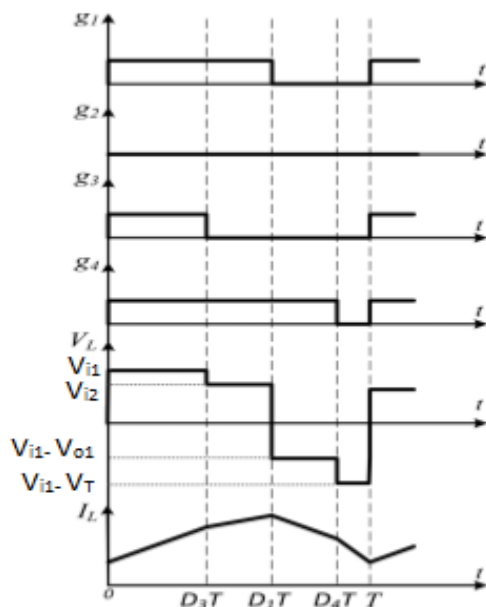


Figure 2 Discharging waveform of non isolated converter

According to the states of the switches, there are

### 2.1.1 Switching State 1 ( $0 < t < D_3T$ )

The switches SW1 and SW3 is turned ON, because SW1 is ON, diodes D1 and D2 are reverse biased, so switch SW4 is turned OFF. Since SW3 is ON and  $V_{i1} < V_{i2}$ , diode D0 is reversely biased. The source  $V_{i2}$  charges inductor L, the current in the inductor increases and the capacitors C1 and C2 are discharges and their stored energy is delivered to load resistances R1 and R2, respectively in this state. The equations of the inductor and capacitors in this mode are as follows:

$$\begin{aligned} L \frac{di_L}{dt} &= V_{i2} \\ C_1 \frac{dV_{O1}}{dt} &= -\frac{V_{O1}}{R_1} \\ C_2 \frac{dV_{O2}}{dt} &= -\frac{V_{O2}}{R_2} \end{aligned} \quad (1)$$

### 2.1.2 Switching state 2 ( $D_3T < t < D_1T$ )

The switch SW1 is still ON and SW3 is turned OFF in this mode. As SW1 is ON, diodes D1 and D2 are reverse biased, so switch SW4 is still OFF. The  $V_{i1}$  charges inductor L, the inductor current increases and the capacitors C1 and C2 are discharged and their stored energy is delivered to the load resistances R1 and R2, respectively in this state. The equations of the inductor and capacitors in this mode are as follows:

$$\begin{aligned} L \frac{di_L}{dt} &= V_{i1} \\ C_1 \frac{dV_{O1}}{dt} &= -\frac{V_{O1}}{R_1} \\ C_2 \frac{dV_{O2}}{dt} &= -\frac{V_{O2}}{R_2} \end{aligned} \quad (2)$$

### 2.1.3 Switching state 3 ( $D_1T < t < D_4T$ )

The switch SW1 is turned OFF and switch SW3 is still OFF and whereas the switch SW4 is also turned ON in this mode. Diode D2 is reverse biased. The inductor L is discharged and its stored energy is delivered to C1 and R1, so inductor current decreases and C1 is charged and C2 is discharged and its stored energy is delivered to load resistance R2 in this mode. The energy storage elements L, C1, and C2 equations in this mode are as follows:

$$\begin{aligned} L \frac{di_L}{dt} &= V_{i1} - V_{O1} \\ C_1 \frac{dV_{O1}}{dt} &= I_L - \frac{V_{O1}}{R_1} \\ C_2 \frac{dV_{O2}}{dt} &= -\frac{V_{O2}}{R_2} \end{aligned} \quad (3)$$

### 2.1.4 Switching state 4 ( $D_4T < t < T$ )

All the three switches are in OFF state in this switching mode. So, the diode D2 is forward biased and the inductor L is discharged and delivers its

stored energy to the capacitors C1, C2, and to the load resistances R1 and R2 which in turn charges the capacitors C1 and C2. The equations for inductor and capacitors in this mode are as follows:

$$\begin{aligned} L \frac{di_L}{dt} &= V_{i1} - (V_{O1} + V_{O2}) \\ C_1 \frac{dV_{O1}}{dt} &= I_L - \frac{V_{O1}}{R_1} \\ C_2 \frac{dV_{O2}}{dt} &= I_L - \frac{V_{O2}}{R_2} \end{aligned} \quad (4)$$

## 2.2 Second Operation Mode - Battery Charging Mode (BCM)

In this mode of operation, the source  $V_{i1}$  supplies the load and also delivers the power to  $V_{i2}$  (battery), when the load power is less and battery is required to be charged. The switches SW1, SW2, and SW4 are active and switch SW3 is completely in OFF state. Like previous operating mode of the converter the specific operation is considered for each switch in this mode. To regulate total output voltage  $V_T = V_{O1} + V_{O2}$  to desired value, the switch SW1 is switched and the duty of the switch SW2 is to regulate the battery charging current ( $I_b$ ) to desired value. The switch SW4 controls the output voltage  $V_{O1}$ . It is clearly understood that by regulating the voltage  $V_T$  and  $V_{O1}$ , the output voltage  $V_{O2}$  is also regulated. Gate signals, voltage and current waveforms of switches and inductor are shown in Figure 3. According to the states of the switches, there are four different operating modes in one switching period as follows:

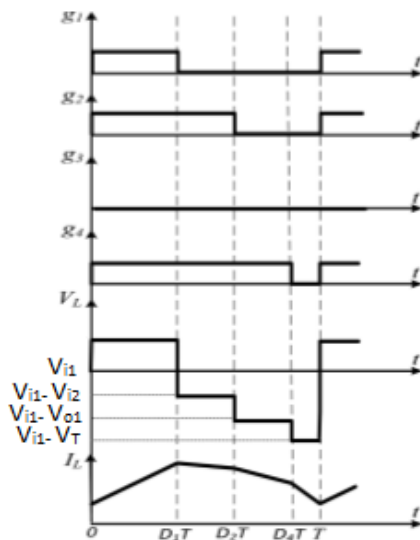


Figure 3 Discharging waveform of non isolated converter

According to the states of the switches, there are four different operation modes in one switching period as follows: Switching State 1 ( $0 < t < D_1T$ ) The switches SW1 and SW3 are turned ON, because SW1 is ON, diodes D1 and D2 are reverse biased, so switch SW4 is turned OFF. Since SW3 is ON and  $V_{i1} < V_{i2}$ , diode D0 is reversely biased. The source  $V_{i2}$

charges inductor L, the current in the inductor increases and the capacitors C1 and C2 are discharged and their stored energy is delivered to load resistances R1 and R2, respectively in this state. The equations of the inductor and capacitors in this mode are as follows:

$$\begin{aligned} L \frac{di_L}{dt} &= V_{i2} \\ C_1 \frac{dV_{O1}}{dt} &= -\frac{V_{O1}}{R_1} \\ C_2 \frac{dV_{O2}}{dt} &= -\frac{V_{O2}}{R_2} \end{aligned} \quad (5)$$

### 2.2.1 Switching State 2 ( $D_1T < t < D_1T$ )

The switch SW1 is still ON and SW3 is turned OFF in this mode. As SW1 is ON, diodes D1 and D2 are reverse biased, so switch SW4 is still OFF. The  $V_{i1}$  charges inductor L, the inductor current increases and the capacitors C1 and C2 are discharged and their stored energy is delivered to the load resistances R1 and R2 respectively in this state. The equations of the inductor and capacitors in this mode are as follows:

$$\begin{aligned} L \frac{di_L}{dt} &= V_{i1} \\ C_1 \frac{dV_{O1}}{dt} &= -\frac{V_{O1}}{R_1} \\ C_2 \frac{dV_{O2}}{dt} &= -\frac{V_{O2}}{R_2} \end{aligned} \quad (6)$$

### 2.2.2 Switching State 3 ( $D_1T < t < D_4T$ )

The switch SW1 is turned OFF and switch SW3 is still OFF and whereas the switch SW4 is also turned ON in this mode. Diode D2 is reverse biased. The inductor L is discharged and delivers its stored energy to C1 and R1, so inductor current decreases and C1 is charged and C2 is discharged and its stored energy is delivered to load resistance R2 in this mode. The energy storage elements L, C1, and C2 equations in this mode are as follows:

$$\begin{aligned} L \frac{di_L}{dt} &= V_{i1} - V_{O1} \\ C_1 \frac{dV_{O1}}{dt} &= I_L - \frac{V_{O1}}{R_1} \\ C_2 \frac{dV_{O2}}{dt} &= -\frac{V_{O2}}{R_2} \end{aligned} \quad (7)$$

### 2.2.3 Switching State 4 ( $D_4T < t < T$ )

All the three switches are in OFF state in this switching mode. So, the diode D2 is forward biased and the inductor L is discharged and delivers its stored energy to the capacitors C1, C2, and to the load resistances R1 and R2 which in turn charges the capacitors C1 and C2. The equations for inductor and capacitors in this mode are as follows:

$$\begin{aligned} L \frac{di_L}{dt} &= V_{i1} - (V_{O1} + V_{O2}) \\ C_1 \frac{dV_{O1}}{dt} &= I_L - \frac{V_{O1}}{R_1} \end{aligned} \quad (8)$$



$$C_2 \frac{dV_{O2}}{dt} = I_L - \frac{V_{O2}}{R_2}$$

### 3. SLIDING MODE CONTROL ELECTRICAL DESCRIPTION

To control the output voltage of the bidirectional boost converter with the output filter is the main aim of the sliding-mode control that is proposed in this article. In other words it is the EV traction system's high voltage DC bus. Regulating the output voltage of the converter regardless of the operation mode and implements a seamless transition is the main purpose of the sliding-mode control. The dynamics of the input current is dominated by the fast motion of the bidirectional boost converter and the slow motion is dominated by the output voltage as in most of the DC/DC converters. The structure of the cascade control regulates the input current with the help of inner loop whereas the outer loop regulates the output voltage

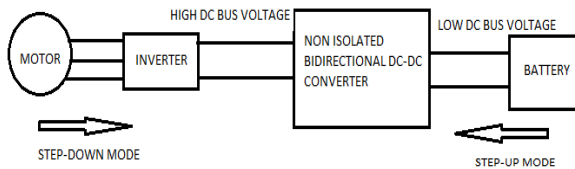


Figure 4 Block diagram of EV traction system with non isolated bidirectional DC-DC converter

This control method can be operated in two operating modes say step-up and step-down modes of the converter are described in the Figure5a and Figure5b. The set-up operation is described in Fig5a. The resistor R0 represents the power delivery of the battery is to the load drive. Therefore, the motor acts as a generator and is modeled with the help of  $V_i$  and is shown in Figure 5b.

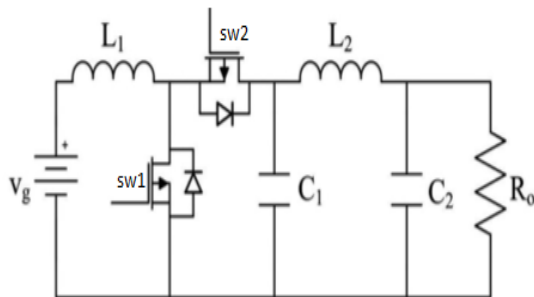


Figure 5a Step down mode of operation

The feasibility of a unique sliding-mode control for this bidirectional converter is studied by analyzing the step-up and step-down operations. Defining state-space variables and their derivatives are as follows,

$$y(t) = \begin{bmatrix} I_{L1}(t) \\ I_{L2}(t) \\ V_{C1}(t) \\ V_{C2}(t) \end{bmatrix}; \quad \dot{y}(t) = \begin{bmatrix} \dot{I}_{L1}(t) \\ \dot{I}_{L2}(t) \\ \dot{V}_{C1}(t) \\ \dot{V}_{C2}(t) \end{bmatrix} \quad (9)$$

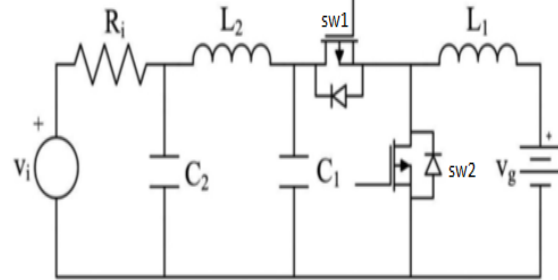


Figure 5b Step up mode of operation

#### 3.1 Step-Up Mode

The calculation of the equivalent control  $U_{eq}$  is made according to the following

$$U_{eq} = -\frac{\nabla S(y(t)), A \cdot y(t) + \delta}{\nabla S(y(t)), B \cdot y(t) + \gamma} = \frac{V_{C1}(t) - V_g}{V_{C1}(t)} \quad (22)$$

The following dynamic equations, that are derived from Equation (11) determines the stability of the system during step-up operation.

$$\dot{I}_{L1}(t) = 0 \quad (23)$$

$$\dot{I}_{L2} = \frac{1}{L_2} V_{C1}(t) - \frac{1}{L_2} V_{C2}(t) \quad (24)$$

$$\dot{V}_{C1}(t) = \frac{1 - U_{eq}(t)}{C_1} - \frac{1}{C_1} I_{C2}(t) \quad (25)$$

$$\dot{V}_{C2}(t) = \frac{1}{C_2} I_{L2}(t) - \frac{1}{R_0 C_2} V_{C2}(t) \quad (26)$$

These equations are corresponds to a third order system. The addition of a single mode current control causes the order reduction and in turn regulates  $I_L$ . Therefore, Equation (24) to Equation (26) is used to calculate characteristics polynomial.

$$P_{SU} = \frac{-1}{L_2 C_1 C_2 R_0} (\lambda^3 L_2 C_1 C_2 R_0 + \lambda^2 L_2 C_1 + \lambda(C_1 + C_2)R_0 + 1) \quad (27)$$

It is proved that the system is stable as long as  $R_0$  is positive through the study of characteristics polynomial

#### 3.2 Step-Down Mode

The equivalent control  $U_{eq}$  is

$$U_{eq} = -\frac{\nabla S(y(t)), A \cdot y(t) + \delta}{\nabla S(y(t)), B \cdot y(t) + \gamma} \quad (28)$$

The step-down mode dynamic equation is given by

$$\dot{I}_{L1}(t) = 0 \quad (29)$$

$$I_{L2} = \frac{1}{L_2} V_{C1}(t) - \frac{1}{L_2} V_{C2}(t) \quad (30)$$

$$\dot{V}_{C1}(t) = \frac{1-U_{eq}(t)}{C_1} - \frac{1}{C_1} I_{C2}(t) \quad (31)$$

$$\dot{V}_{C1}(t) = \frac{1}{C_2} I_{L2}(t) - \frac{1}{R_i C_2} V_{C2}(t) + \frac{1}{R_i C_2} V_i(t) \quad (32)$$

The characteristic polynomial for the step-up mode operation by following the same procedure is,

$$P_{SD} = \frac{-1}{L_2 C_1 C_2 R_i} (\lambda^3 L_2 C_1 C_2 R_i + \lambda^2 L_2 C_1 + \lambda(C_1 + C_2) R_i + 1) \quad (33)$$

Note that the replacement of  $R_o$  by  $R_i$  is the only difference between the Equation (33) and Equation (27). When  $R_i$  is greater than zero, the converter operation during step-down mode will be stable similar to the step-up mode. The chosen converter is enabled by a constant current sliding mode that is regardless of the direction of the power flow

#### 4. COMPARISON OF THE CBB-CM and CBB-IM

The comparisons of the CBB-CM and CBB-IM converter topologies are done based on the following parameters 1) mechanism of the switch; 2) switches and diodes stresses; 3) passive components ratings; 4) passive components size; 5) interleaving capability; and 6) multi-input and multi-output capability.

##### 4.1 Switching Mechanism

Both CBB-CM and CBB-IM converters require only one switch basically, which is to be switched at a particular frequency to operate either as buck or boost converter. For the full switching period of current conduction, the other switch is required to be in the ON state [13]. For maintaining a particular intermediate voltage for CBB-CM, both switches should be switched with different duty ratios, an alternative strategy for this issue appears in [14]; CM can be used as a multi-output converter as this strategy results in a higher intermediate voltage across the central capacitor.

##### 4.2 Rating and switch size

The major concerns when going for final implementation of the converters is Stress on the switches. Switch ratings are largely dependent on the size of the equipment, weight, and cost. The basic single-input single-output converter configuration requires four power switches along with freewheeling diodes. The peak voltage across any switch for the CBB-IM depends on the operation.

All of the switches and diode experience the same voltage stress in CBB-CM, which equals the voltage across the center capacitor. The maximum voltage across the center capacitor must be limited to the value that the switches are designed to withstand.

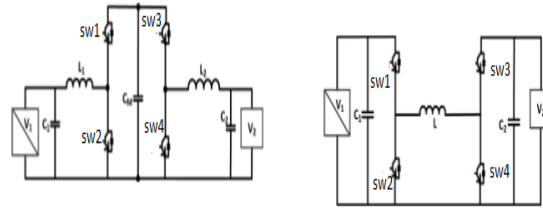


Figure 6 CBB-CM and CBB-IM

##### 4.3 Inductor and Capacitor Ratings and Sizes

The passive element which is used in any high-power converters are inductors, they are the largest and expensive elements. The selection of one topology over the other is strongly influenced by the inductor size. CBB-IM requires only one inductor, whereas CBB-CM requires two as shown in Figure6. For the final selection of the converter, sizes and rating of the inductor must be calculated. The rating of the inductor depends on the operating condition in case of both the converters. The average current through the inductor for CBB-IM, largely depends on the operating mode and operating voltages at any side.

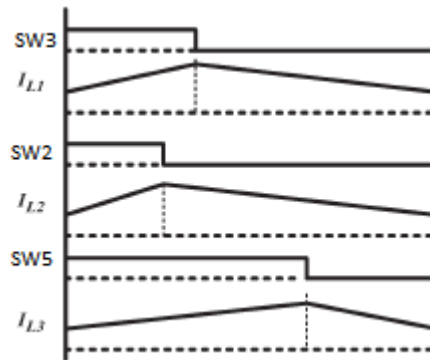


Figure 7 Boost mode and buck mode of CBB-CM

##### 4.4 Multiple-Inputs and Outputs

A dc-dc converter that uses multiple input sources or requires multiple auxiliary outputs with multi-input and multi-output capability is required for EV. Two sources such as an ultra capacitor and a battery pack combination are needed to be connected Multiple input options are required [15]–[17]. Now a day, to reduce emissions and improve gas mileage, the mechanical engine belt compressor has been replaced by an electrical driven compressor for air conditioning systems. The electrically driven compressor motor is driven by a high voltage (220–400 V) at 3–5-kW power requirements [18]–[19]. The use of CBB-CM and CBB-IM topologies with multi-input and multi-output is analyzed in the following. The CBB-CM topology with auxiliary outputs connected to  $V_{o1}$  and  $V_{o2}$  is shown in Figure7.

The gate switching signals and the duty cycles  $D_2$ ,  $D_3$ , and  $D_5$  for of SW2, SW3, and SW5, can be represented with respect to port voltages

$$D2 = 1 - \frac{V_C}{V_i}$$

$$D3 = 1 - \frac{V_{O1}}{V_C}$$

$$D5 = 1 - \frac{V_O}{V_C}$$

The CBB-CM converter can also be used in Vehicle to Grid operation with the battery pack and ultra capacitor bank serving as multiple input sources and with an external dc load connected across C4 at VO as shown in Figure 6. For Vehicle to Grid mode of operation, C4 port connects the inverter to the grid. The gate switching signals and the duty cycles D2, D4, and D5 for of SW2, SW4, and SW5, are

$$D2 = 1 - \frac{V_C}{V_{i1}}$$

$$D4 = 1 - \frac{V_C}{V_{i2}}$$

$$D5 = 1 - \frac{V_O}{V_C}$$

where VC is the intermediate voltage

The CBB-CM converter can also be used in the Grid to Vehicle charging mode, multi-output are served with the help of battery pack and ultra capacitor bank. The charging port C4 is connected to a dc source, C1 and C2 ports are used for charging of battery or ultra capacitor.

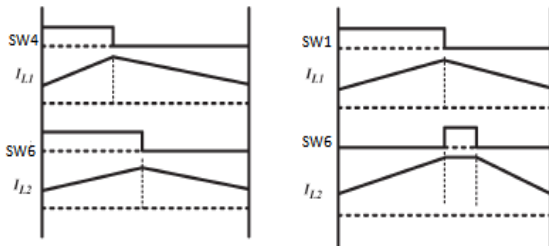


Figure 8 Boost and buck mode in CBB-IM

Similar to the CBB-CM topology, the CBB-IM converter can be used with one input and multi-output. The duty cycles D4 and D6 for the gate switching signals of SW4 and SW6, respectively, are

$$D4 = 1 - \frac{V_i}{V_{O1}}$$

$$D6 = 1 - \frac{V_i}{V_{O2}}$$

In CBB-IM topology, control of the gate signal is complex for certain operating modes. An extra freewheeling mode is required in case of multiple output buck operation for the lower output branch as shown in Figure 8.

## 5. SIMULATION RESULTS

In simulations, input source 2 is used as battery model. The output voltages of the converter are

desired to be regulated on  $V_{O1}$ ,  $V_{O2}$ . Consequently, total output voltage is desired to be regulated on  $V_T$ . Also, output current  $I_o$  is desired is regulated or battery discharging and charging modes, respectively. The battery discharging mode of the converter is investigated in the beginning. In this mode switches SW1, SW2 and SW3 active.

The output voltages  $V_{O1}$  and  $V_T$  are regulated to the desired values. The source 1 in addition to supply the loads delivers power to source 2 and the switches S1 , S2 , and S4 are active in battery charging mode, desired values of output voltages  $V_{O1}$ ,  $V_{O2}$  and  $I_o$  output current is shown in Figure9.a. In Figure9.b.the output current and voltage of the bidirectional boost converter with filter is shown. The multi-output case for the CBB-IM is considered the same as that of the CBB-CM for the simulation. The results in Figure 10 show a satisfactory operation of the Multi- input CBB-CM topology. The result in Figure11 shows a satisfactory operation of the multiple outputs CBB-IM topology.

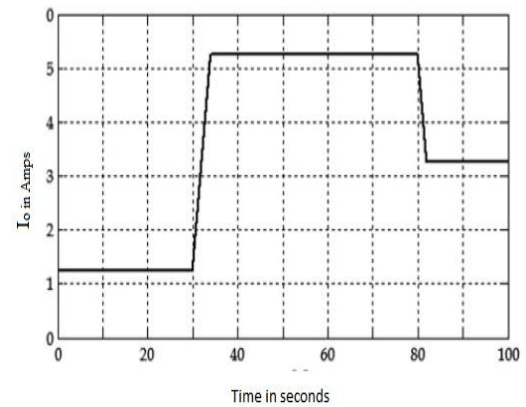


Figure 9a Output current of the bidirectional converter

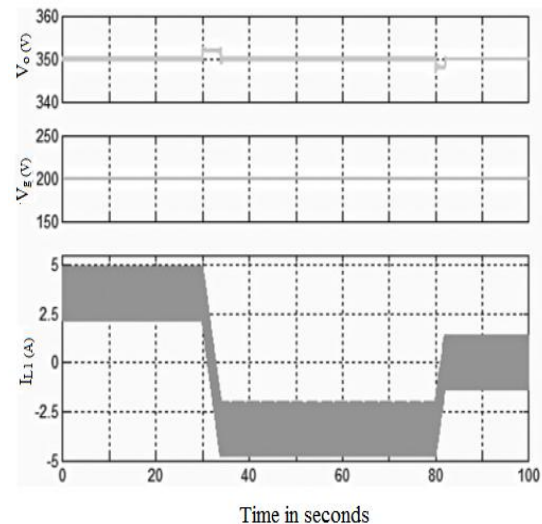


Figure 9b Output current and voltage of the bidirectional boost converter with filter

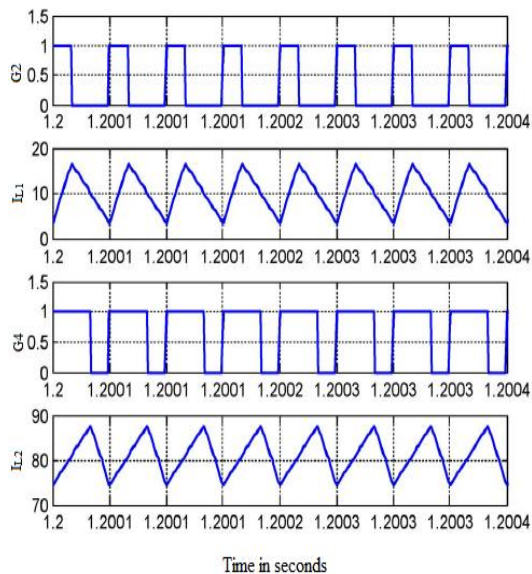


Figure 10 Results for CBB-CM with multi-inputs (Vehicle to Grid mode)

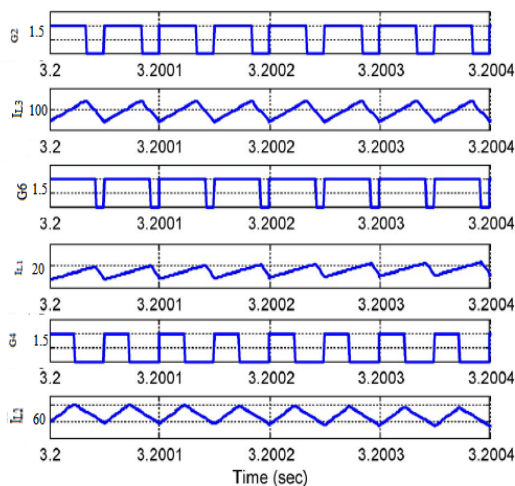


Figure 11 Results for CBB-IM with multi-inputs (Grid to Vehicle mode)

## 6. CONCLUSION

Each converter has its own advantages over the other in certain aspects. Efficiency analysis has been carried out and its output voltage and current are analyzed in Electric vehicle applications. The proposed non isolated multi-input multi-output converter has one inductor. For transferring energy between different energy resources such as FC, PV, and ESBSs like battery and SC, this converter can be used. In this paper, FC and battery are considered as power source and ESBS.

During the discharging mode of the converter, both of input sources deliver power to output source and in the battery charging mode of the converter one of the input sources supplies loads and also delivers power to the other battery. The stability of the converter has been proven for a current and voltage using a

seamless sliding mode control. This control technique gives the unconditional stability of the converter under the sliding motion in both charging and discharging modes. To damp the resonance of the LC tank, an RC network has been added and it ensures the smooth transition between the modes of operation.

Several outputs with different voltage levels are possible with non isolated multi-input multi-output converter, so this converter is best suitable for single-input multi-output converter applications. The input-side and output-side controls are independent for CBB-CM, so it has a better performance in case of multi-input and multi-output applications. System control flexibility and reliability requires fewer components in case of CBB-IM, on the other hand it is better with CBB-CM.

## REFERENCES

- [1] X. Zhang and C. Mi, Vehicle Power Management, New York, NY, USA: Springer, 2011.
- [2] M. Ehsani, Y. Gao, and A. Emadi, Modern Electric, Hybrid Electric and Fuel Cell Vehicle Fundamentals, Theory and Design, 2nd ed., New York, NY, USA: CRC Press, 2010.
- [3] R. Ahmadi and M. Ferdowsi, "Double-input converter on h-bridge cells: derivation, small-signal modeling, and power sharing analysis" IEEE Trans. Circuit Syst., vol. 59, no. 4, pp. 875–889, Apr. 2012.
- [4] V. A. K.Prabhala, D.Somayajula and M. Ferdowsi, "Power sharing in a double-input buck converter using dead-time control," in Proc. Energy Convers. Congr. Expo., 2009.
- [5] Z. Liu, O. Onar, and A. Khaligh, "Design and control of a multiple input DC/DC Converter for battery/ultra capacitor based electric vehicle power system" in Proc. IEEE Twenty-Fourth Annu. Appl. Power Electron. Conf. Expo., 2009.
- [6] K. Gummi and M. Ferdowsi, "Double-input DC-DC power electronic converters for electric-drive vehicles –topology exploration and synthesis using a single-pole triple-throw switch," IEEE Trans. Ind. Electron., vol. 57, no. 2, pp. 617–621, Feb. 2010.
- [7] S.M.Dehghan, M.Mohamadian, A.Yazdian and F.Ashrafzadeh, "Dual input dual-output Z-source inverter," IEEE Trans. Power Electron., vol.25, no. 2, pp. 360–368, Feb. 2010.
- [8] T. Bhattacharya, V. S. Giri, K. Mathew, and L. Umanand, "Multiphase bidirectional flyback converter topology for hybrid electric vehicles," IEEE Trans. Ind. Electron., vol. 56, no. 1, pp. 78–83, Jan. 2009.
- [9] Barrado, J.A., El Aroudi, A., Valderrama-Blavi, H., Calvente, J., Martinez-Salamero, L.: 'Analysis of a self-oscillating bidirectional dc-dc converter in battery energy storage applications', IEEE Trans. Power Deliv., 2012, 27, (3), pp. 1292–1300
- [10] F. Caricchi, F. Crescimbeni, F. G. Capponi, and L. Solero, "Study of bidirectional buck-boost converter topologies for application in electrical vehicle motor drives," in Proc. IEEE APEC Expo., Feb. 1998, vol. 1, pp. 287–293.
- [11] R.M. Schupbach and J. C. Balda, "Comparing dc-dc converters for power management in hybrid electric vehicles," in Proc. IEEE IEMDC, Jun. 1–4, 2003, vol. 3, pp. 1369–1374.
- [12] D. Yu, Z. Xiaohu, B. Sanzhong, S. Lukic, and A. Huang, "Review of nonisolated bi-directional dc-dc converters for plug-in hybrid electric vehicle charge station application at municipal parking decks," in Proc. IEEE APEC Expo., Feb. 2010, pp. 1145–1151.
- [13] S.Waffler and J.W.Kolar, "A novel low loss modulation strategy for high power bidirectional buck+boost converters," IEEE Trans. Power Electron, vol. 24, no. 6, pp. 1589–1599, Jun. 2009.
- [14] M.A.Khan, I.Husain and Y.Sozer, "A bidirectional dc-dc converter with overlapping input and output voltage ranges



- and vehicle to grid energy transfer capability,” IEEE J. Emerging Sel. Topics Power Electron., vol. 2, no. 3, pp. 507–516, Sep. 2014.
- [15] M. B. Camara, H. Gualous, F. Gustin, and A. Berthon, “Design and new control of dc/dc converters to share energy between supercapacitors and batteries in hybrid vehicles,” IEEE Trans. Veh. Technol., vol. 57, no. 5, pp. 2721–2735, Sep. 2008.
- [16] A. Khaligh and L. Zhihao, “Battery, ultracapacitor, fuel cell, hybrid energy storage systems for electric, hybrid electric, fuel cell, plug-in hybrid electric vehicles: State of the art,” IEEE Trans. Veh. Technol., vol. 59, no. 6, pp. 2806–2814, Jul. 2010.
- [17] R. de Castro et al., “Robust dc-link control in EVs with multiple energy storage systems,” IEEE Trans. Veh. Technol., vol. 61, no. 8, pp. 3553–3565, Oct. 2012.
- [18] Electric Vehicle News, Jun. 21, 2009. [Online]. Available: <http://www.electric-vehicle-news.com/> [19] P.-H. Lin, “Performance evaluation and analysis of EV air-conditioning system,” World Elect. Veh. J., vol. 4, pp. 197–201, Nov. 2010.
- [19] K. Umezu and H. Noyama, “Air-conditioning system for electric vehicles (i-MiEV),” presented at the SAE Automotive Refrigerant System Efficiency Symp., Scottsdale, AZ, USA, 2010.
- [20] Laura Albiol-Tendillo, Enric Vidal-Idiarte, Javier Maixe-Altes, Sylvia Mendez-Prince and Luis Martinez-Salamero, “Seamless sliding-mode control for bidirectional boost converter with output filter for electric vehicles applications,” IET Power Electron., 2015, Vol. 8, Iss. 9, pp. 1808–1816 & the Institution of Engineering and Technology 2015.
- [21] Ali Nahavandi, Mehrdad Tarafdar Hagh, Mohammad Bagher Bannae Sharifian, and Saeed Danyali, “A Nonisolated Multiinput Multioutput DC–DC Boost Converter for Electric Vehicle Applications,” IEEE Transactions on Power Electronics, Vol. 30, No. 4, April 2015.
- [22] Mehnaz Akhter Khan, Adeeb Ahmed, Iqbal Husain, Yilmaz Sozer, and Mohamed Badawy, “Performance Analysis of Bidirectional DC–DC Converters for Electric Vehicles,” IEEE Transactions on Industry Applications, Vol. 51, No. 4, July/August 2015.

### Authors Biography



**J. Ramprabu** works as an Assistant professor in the Department of EEE, Kumaraguru College of Technology. He has an Academic experience of 8 years. He is currently working towards the research in renewable energy and embedded system from the faculty of Anna University, Chennai.

He is a Member of the Indian Society for Technical Education and Member of System society of India.



**K. Deepa** is a PG Scholar in Embedded System Technologies in Kumaraguru College of Technology, Coimbatore. She completed B.E in Electrical and Electronics Engineering from Sri Krishna College of Engineering and

Technology, Coimbatore.